December 1995

Surface-related breakdown in silicon: Imaging of current filaments in long p^+-n^--n^+ structures

B. J. Hankla
University of Nebraska - Lincoln

P. F. Williams
University of Nebraska - Lincoln, pfw@moi.unl.edu

G. A. Frecks
University of Nebraska - Lincoln

F. E. Peterkin
Naval Surface Warfare Center, Code B, Dahlgren, VA

Surface-related breakdown in silicon: Imaging of current filaments in long p^+-n^--n^+ structures

B. J. Hankla, P. F. Williams, G. A. Frecks, and F. E. Peterkin[a)]
Department of Electrical Engineering, University of Nebraska–Lincoln, Lincoln, Nebraska 68588

(Received 26 June 1995; accepted for publication 30 October 1995)

We present Schlieren images which show the existence and evolution of current filaments during the very early stages of surface-related breakdown inside 1 cm silicon p^+-n^--n^+ structures. These images confirm our previous finding that breakdown occurs in the silicon rather than in the ambient, and suggest that a streamerlike mechanism may be responsible. © *1995 American Institute of Physics.*

Surface breakdown in high electric fields often sets the failure threshold for solid state devices. The physical processes leading to the destructive breakdown are not well understood.[1,2] This failure occurs in fields well below the dielectric strength of silicon and is termed ''surface flashover,'' since it frequently is accompanied by a weak visible emission. The high fields can be intentionally applied such as for photoconductive switches,[3–6] or due to unwanted transient fields such as during electrostatic discharge (ESD).[7] Much work has been reported by several groups trying to increase the hold off voltage of silicon.[8–10] Efforts have been primarily aimed at changing various surface and device properties to increase the flashover threshold, but very little progress has been made in understanding the physics. In this letter we provide images of current filaments inside silicon during the early stages of surface related breakdown, which contribute new information about the process.

The research presented in the following sections is an extension of the work by Peterkin and Williams,[2,11–13] who used fast shutter and streak photography to study the visible emission from carefully prepared silicon samples during a breakdown event. They found that for applied fields of 30 kV/cm, forward biased p^+-n^--n^+ devices failed on a typical time scale of 10 ns. Similar n^+-n^--n^+ devices generally withstood higher fields for a given voltage pulse duration. The work concluded that in the early stages of breakdown the majority of the current was flowing inside the semiconductor (implying a solid state breakdown phenomenon) and that the nature of this breakdown was influenced by the type of carriers injected at the contacts.

In this study we have used a different diagnostic to delineate better the physical processes which lead to surface flashover. Our work is centered around the early time development of filamentary structures in the silicon. Our diagnostic is a variation of Schlieren photography[14] and uses an infrared laser beam to view the filaments as they develop inside the silicon.

The silicon samples for this study were fabricated from *n*-type float-zone silcon of resistivity 5–20 kΩ cm. The silicon is fashioned into rectangular prisms 1 cm long (⟨111⟩ direction), 0.8 cm wide, and 0.2 cm thick. The 2.5 cm diameter ingots are first cut into 1 cm thick pucks. Both faces of each puck are mechanically ground on abrasive pads and then chemomechanically lap polished on a commercial finishing pad in a colloidal silica slurry to form a flat, low-damage surface. These surfaces are cleaned and then diffusion-doped heavily *n* or *p* type to depths of approximately 10–15 μm to produce contact junctions for the eventual samples. Each puck is cut into six to eight prisms of the above dimensions and all faces on each prism are ground and polished in the manner described for the puck faces. These prisms are again cleaned, aluminum is evaporated onto the doped surfaces, and the contacts are annealed.

The two junction configurations used for the work reviewed in this letter are p^+-n^--n^+ and n^+-n^--n^+. Low voltage *I–V* curves taken of the devices show the expected rectifying behavior for the p^+-n^--n^+ devices and linear behavior for the n^+-n^--n^+ devices. In forward bias, current densities are as expected for bulk silicon.

Figure 1 is a schematic diagram of the experimental setup. The high voltage is applied to the sample using a laser triggered spark gap (LTSG) system consisting of a high voltage supply usually set to 60 kV, charging cable, spark gap, and 50 Ω matched load. A pulsed nitrogen laser beam fo-

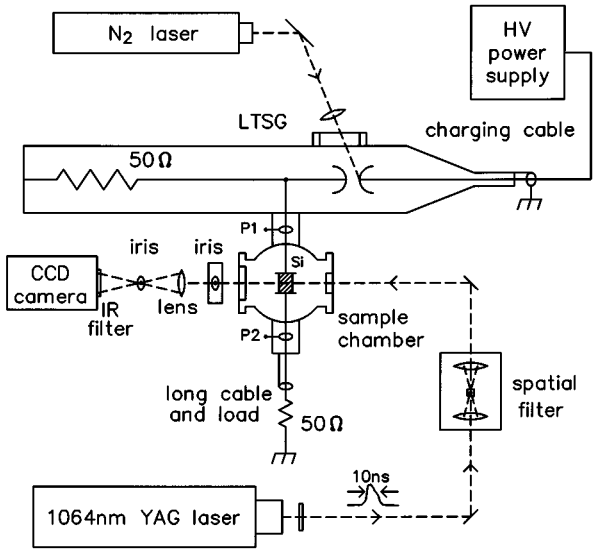

FIG. 1. Schematic diagram of the experimental setup.

[a)]Present address: Naval Surface Warfare Center, Code B, Dahlgren, VA 22448-5100.

 0003-6951/95/67(26)/3942/3/$6.00

cused on one electrode is used to initiate the LTSG arc breakdown. The arc shorts the spark gap and applies half of the charging voltage, 30 kV, to the anode of the sample. For the cable length used here, the pulse duration is approximately 60 ns. The rise time is less than 15 ns. The silicon sample is mounted between spring loaded copper electrodes in a chamber evacuated to less than 8×10^{-7} Torr. The cathode of the sample is connected to a resistive load comprised of a long 50 Ω terminated cable. Capacitively coupled probes at the anode and cathode (points P1 and P2) measure the applied voltage across and, indirectly, the current through the prism during a voltage pulse.

The infrared imaging light source is the fundamental 1064 nm wavelength from a Nd:YAG pulsed laser. The beam is attenuated by several beam splitter stages and a neutral density filter and passed through a spatial filter consisting of an input focusing lens, pinhole, and collimating lens. The filtered beam then is directed into an optical port on the sample chamber, through the silicon sample and out a second chamber port. The beam proceeds through a 1.5 cm diameter iris, an imaging lens, and a 0.2 cm diameter iris located at the imaging lens focus. It is low-pass filtered as it enters a PAR CCD camera equipped with a mechanical shutter and is collected by the silicon CCD array. The iris at the focal point of the imaging lens filters out light which is not collinear with the YAG probe beam. This creates contrast in areas of the image plane corresponding to areas in the sample which refract or diffract the beam. Time resolution is 10 ns as determined by the YAG pulse duration [see Fig. 2(b)]. The apertures and infrared filter strongly attenuate optical emission from the sample, but what gets through is integrated over the 20 μs mechanical shutter open time of the CCD camera.

An example of the current filamentation observed in a p^+-n^--n^+ structure is shown in Fig. 2(a). The 1 cm long prism was forward biased with the anode shown at the left of the photograph. The dark vertical line on the silicon at the cathode is due to an imperfection in the flatness of the polished surface. The small spots along the top edge and in the upper right corner are sample and optical system flaws present in all photographs of this particular sample. The composite oscilloscope trace in Fig. 2(b) shows the current as measured at P2 and the timing of the YAG probe pulse during the event. The ampere values labeled on the graph give the sample current and the YAG pulse intensity is presented in arbitrary units. The arrival of the voltage pulse on the sample is marked by the initial increase of the current at time 0.0 ns. The current then levels out at about 0.5 A, which is what is expected based on the density of carriers and assumed carrier velocity saturation. At approximately 25 ns the current increases rapidly indicating the onset of the breakdown. Often a spike as shown in the trace is seen. The current then continues to increase until it reaches a system impedance limit of about 400 A or the applied voltage is removed. In the photograph there is no evidence of any visible discharge or flashover. This was the case for the majority of the tests with the short 60 ns pulse. Only rarely was any emitted light detected from the p^+-n^--n^+ samples and in those cases it was associated with a spot where two or more

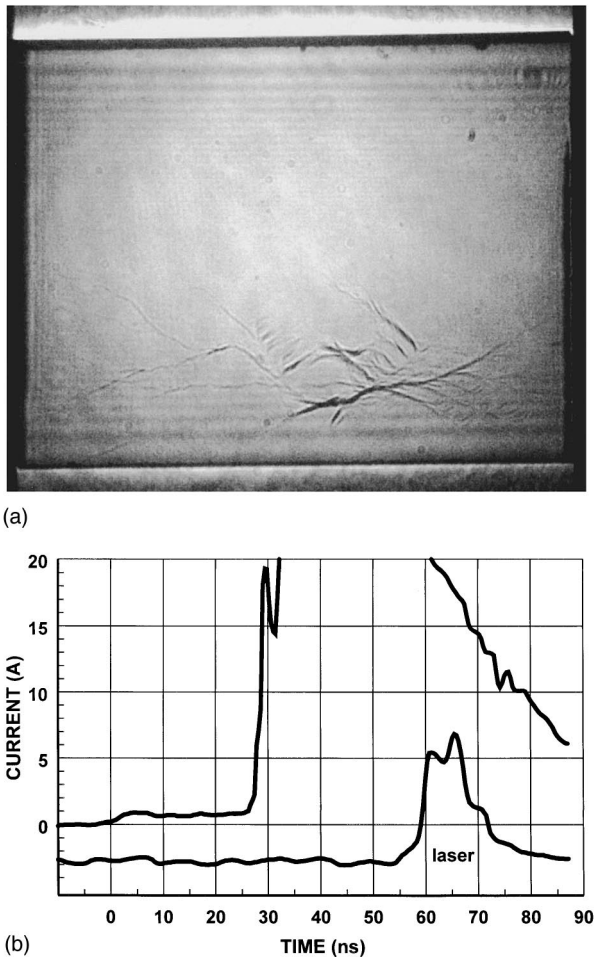

FIG. 2. (a) Photograph showing filaments in a p^+-n^--n^+ silicon device about 35 ns after the start of breakdown. The device length is 1 cm, the applied voltage is 30 kV, and the anode is on the left. (b) Oscilloscope trace of the current through the sample during the shot imaged in (a). The laser trace shows the probe laser intensity and provides timing information.

branches met or occasionally a spot on a straight filament near the cathode.

Referring to the scope trace in Fig. 2(b), the very early time development of the imaged filaments in similar p^+-n^--n^+ prisms becomes visible at approximately 10 ns after the onset of breakdown. They begin as spots in the interior, then branch out quickly during the next 10 ns, darken, and continue to develop into full filaments like those in Fig. 2(a).

No current filamentation was observed in the n^+-n^--n^+ samples during the 60 ns voltage pulse. The current level did not increase abruptly and was consistent throughout the voltage pulse with that expected assuming carrier velocity saturation.

Insight into the nature of the filaments can be obtained through a more quantitative analysis of the data. The structures we see are due primarily to refraction of the parallel rays of the probe laser by variations in the index of refraction in the silicon. By making assumptions about the geometry of the filaments, we can estimate the change in index responsible. For this analysis we assume the filaments have a circular cross section and a uniform index differing from that of

the bulk silicon by Δn. We estimate the Δn required to deflect a typical ray just out the aperture of the iris located in the focal plane of the imaging lens as $\Delta n_{\min} \approx R/f_i$, where R is the radius of the aperture, and f_i is the focal length of the imaging lens. For our setup, $\Delta n_{\min} \approx 0.01$.

Variations in temperature and in electron density can produce index changes. Using the data of Jellison and Modine,[15] a modest temperature change of about 40 °C is required to produce a change of our $\Delta n_{\min}$. Using a simple Drude model,[16] we estimate the Δn produced by an electron density of 10^{18} cm^{-3} to be only about 10^{-4}. On this basis, we conclude that we are seeing temperature variations.

With our assumption that the filament first becomes visible when the temperature has increased by 40 °C, we can estimate the carrier density in the filaments. Assuming a field equal to the applied field of 30 kV/cm, an average carrier density of about 5×10^{16} cm^{-3} would be required to produce this temperature rise in 15 ns. This density is consistent with the measured current during this time. Assuming velocity saturation for both carrier types, the current flowing in a typical channel 0.016 cm in diameter would be 32 A, within a factor of 2 of the typical peak current seen during the first 15 ns of breakdown.

We believe that the filaments we see result from heating in a filamentary channel which was produced by some as yet undetermined mechanism. The formation and/or evolution of these channels is influenced by the characteristics of the contact junction regions. We do not believe that we have seen the initial formation of this channel. Rather, the features we see appear where the time-integrated product of the field and current density is sufficient to raise the temperature of the channel above our detection threshold. The initiation point for the formation of the channels is, then, not necessarily where they first are detectable.

Although our data are not conclusive, we propose that the filaments result from phenomena similar to the streamers seen in atmospheric-pressure gases.[17] The fast current rise occurs when one or more of these ''streamers'' bridges the gap between the electrodes. Since the time to the start of the fast current rise is often less than 30 ns, the ''streamer'' propagation velocity must be greater than 3×10^7 cm/s. This minimum value is three times the 1×10^7 cm/s saturation drift velocity for electrons in silicon,[18] but below typical streamer velocities observed in gases,[19] and well below velocity estimates for streamers in gallium arsenide.[20,21]

This work was supported by the Office of Naval Research under Grant No. N00014-92-J-4028. We thank B. J. Ganguly for providing us with one boule of high resistivity silicon.

[1] C. G. B. Garrett and W. H. Brattain, J. Appl. Phys. **27**, 299 (1956).
[2] F. E. Peterkin, T. Ridolfi, L. L. Buresh, B. J. Hankla, D. K. Scott, P. F. Williams, W. C. Nunnally, and B. L. Thomas, IEEE Trans. Electron. Devices **ED-37**, 2456 (1990).
[3] W. C. Nunnally, *5th IEEE Pulsed Power Conference*, edited by M. F. Rose and P. J. Turchi (IEEE, New York, 1985), pp. 235–241.
[4] G. M. Loubriel, M. W. O'Malley, and F. J. Zutavern, *6th IEEE Pulsed Power Conference*, edited by P. J. Turchi and B. H. Bernstein (IEEE, New York, 1987), pp. 145–148.
[5] E. E. Funk, E. A Chauchard, Chi H. Lee, and M. J. Rhee, Proceedings of the 4th SDIO/ONR Pulse Power Meeting, 1991, pp. 12–22.
[6] D. M. Giorgi, A. H. Griffin, D. E. Hargis, I. A. McIntyre, and O. S. F. Zucker, *8th IEEE Pulsed Power Conference*, edited by R. White and K. Prestwich (IEEE, New York, 1991), pp. 122–125.
[7] R. J. Antinone, *Electrical Overstress Protection for Electronic Devices* (Noyes, Engelwood Cliffs, NJ, 1986).
[8] B. I. Thomas and W. C. Nunnally, in Ref. 4, pp. 149–152.
[9] R. J. Feuerstein and B. Senitzky, J. Appl. Phys. **70**, 288 (1991).
[10] J. M. Elizondo and W. M. Moeny, in Ref. 6, pp. 1020–1023.
[11] P. F Williams and F. E Peterkin, *7th IEEE Pulsed Power Conference*, edited by B. H. Bernstein and J. P. Shannon (IEEE, New York, 1989), pp. 890–892.
[12] F. E Peterkin, P. F. Williams, T. Ridolfi, B. J. Hankla, and L. L. Buresh, in Ref. 6, pp. 118–121.
[13] F. E. Peterkin, P. F. Williams, B. J. Hankla, L. L. Buresh, and S. A. Woodward, Appl. Phys. Lett. **62**, 2236 (1993).
[14] L. A. Vasilev, *Schlieren Methods* (Keter, New York, 1986).
[15] G. E. Jellison, Jr. and F. A. Modine, J. Appl. Phys. **76**, 3758 (1994).
[16] See for example: Charles Kittel, *Introduction to Solid State Physics* (Wiley, New York, 1986).
[17] I. Gallimberti, J. Phys. **40**, C7 (1979).
[18] J. F. Gibbons, IEEE Trans. Electron Devices **ED-14**, 37 (1967).
[19] P. F. Williams and F. E. Peterkin, *Physics and Applications of Pseudosparks*, edited by M. Gundersen and G. Schaefer (Plenum, New York, 1990).
[20] C. D. Capps, R. A. Falk, and J. C. Adams, J. Appl. Phys. **74**, 6645 (1993).
[21] G. M. Loubriel, F. J. Zutavern, H. P. Hjalmarson, R. R. Gallegos, W. D. Helgeson, and M. W. O'Malley, Appl. Phys. Lett. **64**, 3323 (1994).